

# VideoMage: Multi-Subject and Motion Customization of Text-to-Video Diffusion Models

Chi-Pin Huang<sup>1,†</sup>, Yen-Siang Wu<sup>2</sup>, Hung-Kai Chung<sup>2</sup>,  
Kai-Po Chang<sup>1</sup>, Fu-En Yang<sup>3</sup>, and Yu-Chiang Frank Wang<sup>1,3,‡</sup>

<sup>1</sup> Graduate Institute of Communication Engineering, National Taiwan University

<sup>2</sup> National Taiwan University <sup>3</sup> NVIDIA

<sup>†</sup>f11942097@ntu.edu.tw, <sup>‡</sup>frankwang@nvidia.com



Figure 1. **Illustration of multi-subject and motion customization.** Given images of multiple subjects, a reference motion video, and a related text prompt, our *VideoMage* is able to produce video outputs aligned with such inputs.

## Abstract

Customized text-to-video generation aims to produce high-quality videos that incorporate user-specified subject identities or motion patterns. However, existing methods mainly focus on personalizing a single concept, either subject identity or motion pattern, limiting their effectiveness for multiple subjects with the desired motion patterns. To tackle this challenge, we propose a unified framework *VideoMage* for video customization over both multiple subjects and their interactive motions. *VideoMage* employs subject and motion LoRAs to capture personalized content from user-provided images and videos, along with an

appearance-agnostic motion learning approach to disentangle motion patterns from visual appearance. Furthermore, we develop a spatial-temporal composition scheme to guide interactions among subjects within the desired motion patterns. Extensive experiments demonstrate that *VideoMage* outperforms existing methods, generating coherent, user-controlled videos with consistent subject identities and interactions. Project Page: <https://jasper0314-huang.github.io/videomage-customization>

## 1. Introduction

In recent years, unprecedented success in diffusion models [17, 37, 38] has greatly improved the generation of pho-

torealistic videos [3, 16, 18, 19, 35] from textual descriptions, enabling new possibilities for video content creation. However, while high-quality and diverse videos can now be synthesized, relying solely on text descriptions cannot offer precise control over desirable content that accurately aligns with user intents [24]. Therefore, customizing user-specific video concepts from the provided references draws significant attention from both academics and industry.

To address this challenge, several works [14, 24, 43, 44] have explored customizing a desirable *subject identity* into synthesized videos. For example, AnimateDiff [14] animates the user-provided subject by tuning temporal modules inserted into the pre-trained image diffusion models. VideoBooth [24] further employs cross-frame attention to preserve the fine-grained visual appearance of the customized subject. Furthermore, CustomVideo [43] fine-tunes cross-attention layers on all involved subjects simultaneously to customize multiple subjects within a scene. However, these approaches merely focus on the customization of the *static subject*. They are limited to offering users or video creators the ability to personalize their desired *dynamic motions* (e.g., specific dancing styles) into output videos, severely hampering the flexibility of video content customization.

On the other hand, to empower the users with the controllability of *dynamic motion*, recent methods [23, 28, 32, 48, 51] have designed modules to capture motion patterns from the conditioned reference videos. For instance, Customize-A-Video [32] fine-tunes low-rank adaptation (LoRA) [21] inserted into temporal attention layers to learn the desired motion pattern. Similarly, MotionDirector [51] employs LoRA to learn motion by using an objective that captures the differences between an anchor frame and the other frames. However, simply tuning temporal modules without properly disentangling motion information from reference videos causes severe *appearance leakage* issues, resulting in the derived motion patterns that cannot be applied with arbitrary subject identities. Moreover, without guidance for subjects and motion *composition*, the model struggles to precisely control the interaction among these customized video concepts. As a result, the aforementioned methods can only handle *single* (i.e., subject or motion) concept customization. Jointly customizing *multiple* video concepts by free-form prompts that describe multiple subjects *and* desired motion patterns remains a challenging and unsolved problem.

In this paper, we propose *VideoMage*, a unified framework for video content customization that enables controllability over subject identities and motion patterns. *VideoMage* involves subject and motion LoRAs to capture respective information from user-provided images and videos. To ensure the motion LoRAs would not be contaminated by visual appearance, we introduce an appearance-agnostic motion learning approach, which isolates motion patterns from reference videos. More specifically, we employ negative classifier-

free guidance [12, 22] conditioned on the visual appearance, effectively disentangling motion from appearance details. With the learned subject and motion LoRAs, we introduce a spatial-temporal collaborative composition scheme to guide interactions among multiple subjects in the desired motion pattern. We advance gradient-based fusion and spatial attention regularization to absorb the multi-subject information while encouraging distinct spatial arrangements of subjects. By iteratively guiding the generation process using subject and motion LoRAs, *VideoMage* synthesizes output videos with enhanced user control and spatiotemporal coherence.

We now summarize the contributions of this work below:

- We propose *VideoMage*, a unified framework that first enables video concept customization for multiple subject identities and their interactive motion.
- We introduce a novel appearance-agnostic motion learning by advancing negative classifier-free guidance to disentangle underlying motion patterns from appearance.
- We develop a spatial-temporal collaborative composition scheme to compose the obtained multi-subject and motion LoRAs for generating coherent multi-subject interactions in the desired motion pattern.

## 2. Related Works

### 2.1. Text-to-Video Generation

Recently, text-to-video generation has made remarkable progress. It has evolved from early approaches based on Generative Adversarial Networks (GANs) [34, 36, 40, 41] and autoregressive transformers [20, 45, 46, 49] to recent diffusion models [3, 7, 18, 19, 35, 42], which have significantly improved both the quality and diversity of generated videos. Pioneering works such as VDM [19] and Imagen-Video [18] modeled video diffusion processes in pixel space, while LVDM [16] and VideoLDM [3] modeled in latent space to optimize computational efficiency. To overcome the challenge of lacking paired video-text data, Make-A-Video [35] utilizes a text-to-image prior to achieve text-to-video generation. On the other hand, open-source models like VideoCrafter [7], ModelScopeT2V [42], and ZeroScope [39] incorporate spatiotemporal blocks to enhance text-to-video generation, demonstrating notable capabilities for producing high-fidelity videos. These powerful text-to-video diffusion models have driven advancements in customized content generation.

### 2.2. Video Content Customization

**Subject Customization.** In recent years, customized generation has gained considerable attention, particularly in image synthesis [11, 26, 33]. Building on these advances, recent efforts have increasingly focused on video subject customization [6, 8, 14, 24, 43, 44], which is more challenging due to the need for generating subjects in dynamic

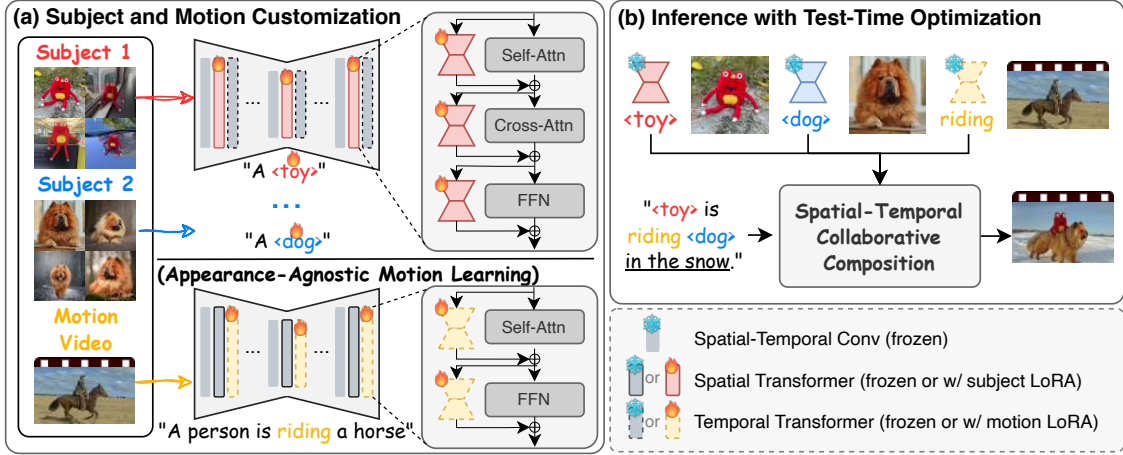


Figure 2. **Overview of VideoMage.** (a) Given images of multiple subjects and a reference video with desirable motion, *VideoMage* advances LoRAs to capture the knowledge of *visual appearances* and *appearance-agnostic motion* information, respectively. (b) With a text prompt relating the aforementioned visual and motion concepts, our *spatial-temporal collaborative composition* refines the input noisy latent  $x_t$  for generating videos matching the desirable visual and motion information.

scenes. For example, AnimateDiff [14] inserts additional motion modules into pre-trained image diffusion models, enabling the animation of custom subjects. Furthermore, VideoBooth [24] employs cross-frame attention mechanisms to preserve the fine-grained visual appearance of the customized subject. Recently, CustomVideo [43] fine-tunes the cross-attention layers on all involved subjects to achieve multi-subject customization. However, these methods tend to produce slight subject movements [44, 47], lacking the controllability by users to enable precise control over motion.

**Motion Customization.** Given a few reference videos describing a target motion pattern, motion customization [23, 28, 32, 44, 48, 51] aims to generate videos that replicate the target motion. For instance, Customize-A-Video [32] fine-tunes low-rank adaptation (LoRA) [21] integrated into temporal attention layers to capture specific motion patterns from reference videos. Similarly, MotionDirector [51] learns motion by fine-tuning LoRA to capture the differences between an anchor frame and the other frames, effectively transferring dynamic behaviors into the generated video content. Very recently, DreamVideo [44] explores the customization of a single subject performing specific motions by employing ID and motion adapters, which are separately appended to the spatial and temporal layers. However, the appearance leakage issue and the lack of proper guidance for subject and motion composition hamper these methods from generating videos with multiple subjects interacting. Thus, the flexibility of customizing video content with arbitrary subjects and motion patterns is strictly limited. To empower users with enhanced controllability over video concepts of subject and motion, we employ a unique *VideoMage* framework to en-

able desired interactions among multiple customized subject identities.

### 3. Method

**Problem Formulation.** We first define the setting and notations. Given  $N$  subjects, each represented by 3-5 images denoted as  $x_{s,i}$  for the  $i$ -th subject (omitting the individual image index for simplicity), a reference interactive motion video  $x_m$ , and a user-provided text prompt  $c_{tgt}$ , our goal is to generate a video based on  $c_{tgt}$  in which these  $N$  subjects interact according to the motion pattern.

To tackle the above problem, we propose *VideoMage*, a unified framework for customizing multiple subjects and interactive motions for text-to-video generation. With a quick review of video diffusion models (Sec. 3.1), we detail how we utilize LoRA modules to learn visual and motion information from input images and reference videos, respectively (Sec. 3.2). Instead of naive combination, a unique spatial-temporal collaborative composition scheme is presented to integrate the learned subjects/motion LoRAs for video generation (Sec. 3.3).

#### 3.1. Preliminary: Video Diffusion Models

Video Diffusion Models (VDMs) [3, 16, 18, 19, 35] are designed to generate video by gradually denoising a sequence of noises sampled from a Gaussian distribution [17]. Specifically, the diffusion model  $\epsilon_\theta$  learns to predict the noise  $\epsilon$  added at each timestep  $t$ , conditioned on the input  $c$ , which is a text prompt in text-to-video generation. The training objective is simplified to a reconstruction loss:

$$\mathcal{L} = \mathbb{E}_{x,\epsilon,t} \left[ \|\epsilon_\theta(x_t, c, t) - \epsilon\|_2^2 \right], \quad (1)$$

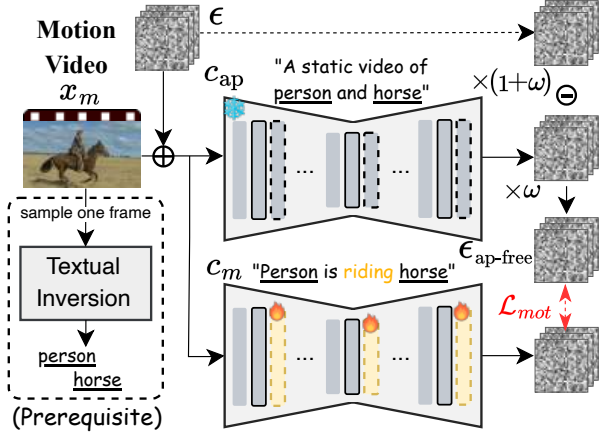


Figure 3. **Appearance-agnostic motion learning.** By utilizing text prompt emphasizing the appearance information (i.e.,  $c_{ap}$ ), we aim to extract appearance-agnostic motion information via the proposed *negative classifier-free guidance*.

where noise  $\epsilon \in \mathbb{R}^{F \times H \times W \times 3}$  is sampled from  $\mathcal{N}(\mathbf{0}, \mathbf{I})$ , timestep  $t \in \mathcal{U}(0, 1)$ , and  $x_t = \sqrt{\bar{\alpha}_t}x + \sqrt{1 - \bar{\alpha}_t}\epsilon$  is the noisy input at  $t$ , with  $\bar{\alpha}_t$  being a hyperparameter for controlling the diffusion process [17]. To reduce computational cost, most VDMs [7, 16, 42] encode the input video data  $x \in \mathbb{R}^{F \times H \times W \times 3}$  into a latent representation (e.g., derived by a VAE [25]). For simplicity, we continue to use video data  $x$  as the model’s input throughout the paper.

### 3.2. Subject and Motion Customization

**Learning of Visual Subjects.** As illustrated at the top of Fig. 2(a), to capture subject appearance for video generation, we learn a special token (e.g., “<toy>”) and use a subject LoRA ( $\Delta\theta_s$ ) to fine-tune the pre-trained video diffusion model. To avoid interfering with temporal dynamics, the subject LoRA is applied only to the spatial layers of the UNet. The objective is defined as:

$$\mathcal{L}_{sub} = \mathbb{E}_{x_s, \epsilon, t} \left[ \|\epsilon_{\theta_s}(x_{s,t}, c_s, t) - \epsilon\|_2^2 \right], \quad (2)$$

where  $x_s \in \mathbb{R}^{1 \times H \times W \times 3}$  is the subject image,  $\theta_s = \theta + \Delta\theta_s$  denotes the parameters of the pre-trained model with the subject LoRA applied, and  $c_s$  is the prompt containing the special token (e.g., “A <toy>”).

However, fine-tuning with image data alone might result in video diffusion models losing their capability in producing motion information. Following [47], we leverage an auxiliary video dataset  $\mathcal{D}_{aux}$  (e.g., Panda70M [9]) to regularize fine-tuning while preserving the pre-trained motion prior. More precisely, given video-caption pair  $(x_{aux}, c_{aux})$  sampled from  $\mathcal{D}_{aux}$ , the regularization loss is defined as:

$$\mathcal{L}_{reg} = \mathbb{E}_{x_{aux}, \epsilon, t} \left[ \|\epsilon_{\theta_s}(x_{aux,t}, c_{aux}, t) - \epsilon\|_2^2 \right]. \quad (3)$$

Thus, the overall objective is then defined as:

$$\mathcal{L} = \mathcal{L}_{sub} + \lambda_1 \mathcal{L}_{reg}, \quad (4)$$

where  $\lambda_1$  is the hyperparameter that control the weight of regularization loss. Optimizing this objective captures the subject appearance while preserving the motion prior. With our training objective, we are able to allow customization for user-provided subject identities without compromising VDM’s capability. However, the tuned VDM remains challenging in precisely controlling motion patterns from reference videos, restricting user’s flexibility and control.

**Learning of Appearance-Agnostic Motion.** To learn the desired motion pattern from the reference video  $x_m$ , a naive strategy is to fine-tune a motion LoRA and inject it into the UNet’s temporal layers (i.e.,  $\Delta\theta_m$  at the bottom of Fig. 2(a)). However, direct applying the standard diffusion loss in Eq. (1) would result in a *appearance leakage* issue, wherein the motion LoRA inadvertently captures the appearance of subjects from the reference video. This entanglement of subject appearance and motion hinders the ability to apply the learned motion patterns to new subjects.

To address this problem, we propose a novel *appearance-agnostic* objective, as shown in Fig. 3, which effectively isolates motion patterns from the reference video. Inspired by concept erasing methods of [12, 22], we advance *negative classifier-free guidance* conditioned on the visual subject appearances, focusing on eliminating appearance information during motion learning. This would ensure that the motion LoRA focuses exclusively on motion dynamics.

To achieve this, we first learn special tokens for the subjects in the reference video (e.g., “person” and “horse” in Fig. 3) by applying textual inversion [11] on a single frame sampled from the reference video. This captures subject appearance while minimizing motion influence, effectively decoupling appearance from motion. With the above special tokens, we train a motion LoRA using an appearance-agnostic objective that employs negative guidance to suppress appearance information, enabling the motion LoRA to learn motion patterns independently of subject appearances. More specifically, the training objective is defined as:

$$\mathcal{L}_{mot} = \mathbb{E}_{x_m, \epsilon, t} \left[ \|\epsilon_{\theta_m}(x_{m,t}, c_m, t) - \epsilon_{ap-free}\|_2^2 \right] \\ \text{where } \epsilon_{ap-free} = (1 + \omega)\epsilon - \omega\epsilon_{\theta}(x_{m,t}, c_{ap}, t). \quad (5)$$

Note that  $\epsilon_{ap-free}$  is the negatively guided *appearance-free* noise,  $\omega$  is the hyperparameter controlling the guidance strength, and  $c_m$  and  $c_{ap}$  describe the motion and the static subject appearances, respectively (e.g., “Person riding a horse” and “A static video of person and horse”).

By optimizing Eq. (5), motion LoRA learns motion patterns independent of subject appearances. This disentangle-

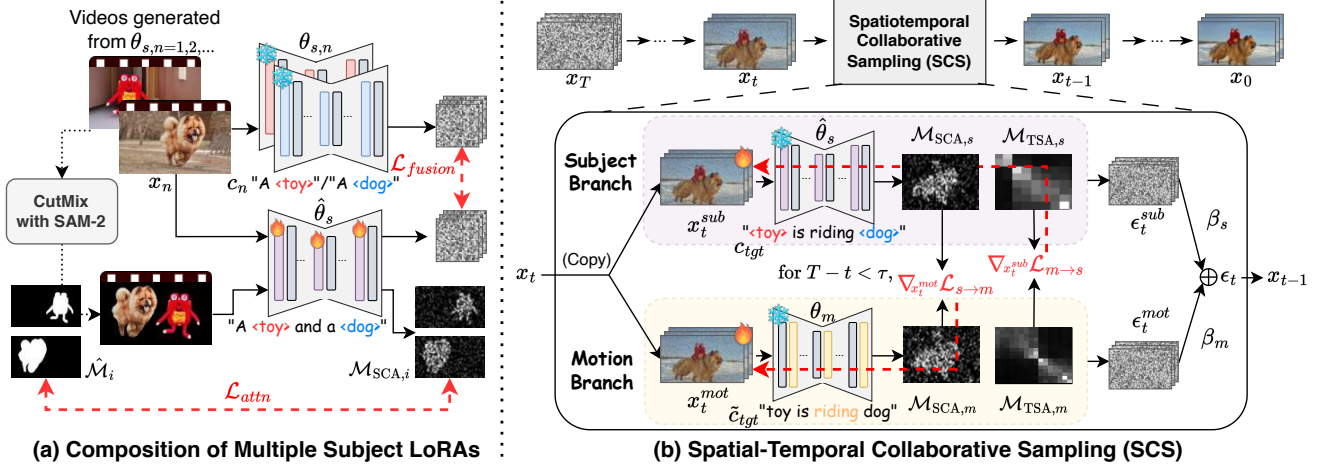


Figure 4. **Spatial-temporal collaborative composition for T2V test-time optimization.** (a) Test-time fusion of subject LoRAs  $\hat{\theta}_s$ , which employs attention regularization  $\mathcal{L}_{attn}$  to ensure appearance preservation of each visual subject. (b) Spatiotemporal Collaborative Sampling (SCS) integrates the fused subject LoRA  $\hat{\theta}_s$  and the motion LoRA  $\theta_m$  by cross-modal alignment, ensuring visual and temporal coherence.

ment is crucial for composing multiple subjects with customized motions, as we will discuss later.

### 3.3. Spatial-Temporal Collaborative Composition

With multiple subject LoRAs and an interactive motion LoRA obtained, our goal is to generate videos where these subjects interact using the desired motion pattern. However, combining LoRAs with distinct properties (i.e., visual appearance vs. spatial-temporal motion) is not a trivial task. In our work, we propose a test-time optimization scheme of *spatial-temporal collaborative composition*, which enables collaboration between the aforementioned LoRAs to generate videos with the desired appearance and motion properties. We now discuss the proposed scheme below.

**Composition of Multiple Subject LoRAs.** We first discuss how we perform fusion of LoRAs describing different visual subject information. We employ gradient-based fusion [13] to distill the distinct identities from each subject LoRA into a single fused LoRA. That is, given multiple LoRAs, denoted as  $\Delta\theta_{s,1}, \Delta\theta_{s,2}, \dots, \Delta\theta_{s,N}$ , where  $N$  is the number of subjects and each LoRA corresponds to a specific subject, our goal is to learn a fused LoRA  $\Delta\hat{\theta}_s$  that is able to generate video featuring multiple subjects.

To achieve this, we aim to enforce the fused LoRA  $\Delta\hat{\theta}_s$  to generate consistent videos with each specific subject LoRA. To be more precise, we optimize  $\Delta\hat{\theta}_s$  by matching the predicted noise between the fused LoRA and the subject-specific one. The multi-subject fusion objective  $\mathcal{L}_{fusion}$  is

formulated as follows,

$$\mathcal{L}_{fusion} = \frac{1}{N} \sum_{n=1}^N \mathbb{E}_{x_n, \epsilon, t} \left[ \|\epsilon_{\hat{\theta}_s}(x_n, t, c_n) - \epsilon_n\|_2^2 \right],$$

where  $\epsilon_n = \epsilon_{\theta_{s,n}}(x_n, t, c_n)$ . (6)

Here,  $x_n$  is the video generated by  $\theta_{s,n}$ , and  $c_n$  is the corresponding prompt for the  $n$ -th subject.

Moreover, to encourage different subject identities to be properly arranged, we further introduce *spatial attention regularization*  $\mathcal{L}_{attn}$  to explicitly guide the model’s attention to focus on the correct subject regions. Specifically, as illustrated in Fig. 4(a), we randomly sample and segment two subjects by Grounded-SAM2 [30, 31], and then combine the segmented subjects into a CutMix-style [15, 50] video. We then formally define  $\mathcal{L}_{attn}$  as:

$$\mathcal{L}_{attn} = \frac{1}{2} \sum_{i=1}^2 \|\mathcal{M}_{SCA,i} - \hat{\mathcal{M}}_i\|_2^2, \quad (7)$$

where  $\mathcal{M}_{SCA,i}$  is the spatial cross-attention map of the  $i$ -th sampled subject, and  $\hat{\mathcal{M}}_i$  is the corresponding ground-truth segmentation mask. Therefore, the overall objective for deriving the multi-subject LoRA is defined as:

$$\mathcal{L} = \mathcal{L}_{fusion} + \lambda_2 \mathcal{L}_{attn}, \quad (8)$$

where  $\lambda_2$  controls the weight of the attention loss. Note that, we only require merging multiple subjects at once. Once the fused LoRA  $\hat{\theta}_s$  is obtained, we are able to generate videos with arbitrary motion patterns, as detailed below.

**Spatial-Temporal Collaborative Sampling (SCS)** To further integrate the motion-based LoRA,  $\Delta\theta_m$ , with the aforementioned fused visual subject LoRA,  $\Delta\hat{\theta}_s$ , we propose a

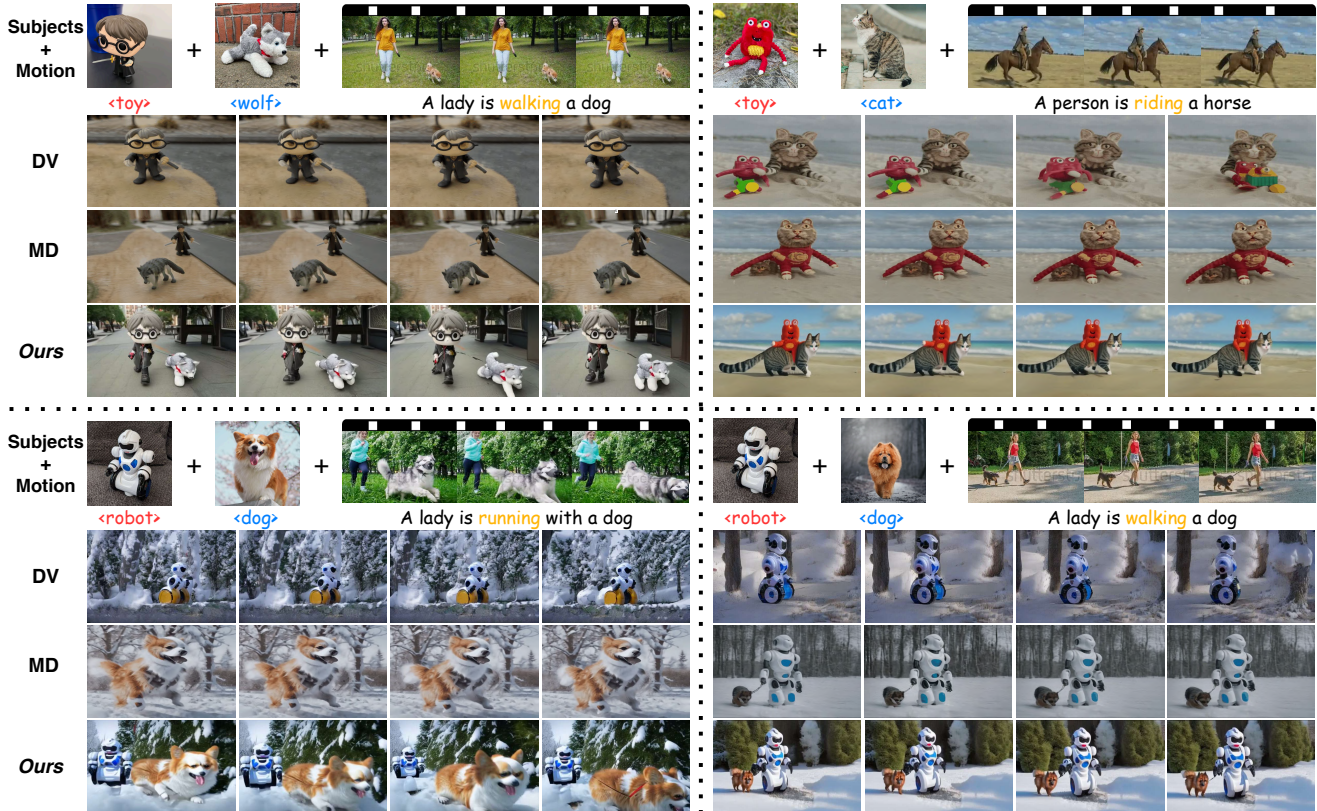


Figure 5. **Qualitative comparisons of different customization methods.** The subject images and the reference motion video are listed at the top of the figure. DV and MD refer to DreamVideo [44] and MotionDirector [51], respectively. Please refer to the supplementary materials for the complete input prompts used for customization (e.g., describing the background, etc.).

novel *spatial-temporal collaborative sampling* (SCS) technique to effectively control and guide interactions among customized subjects. In SCS, we independently sample and integrate noise from the subject branch and the motion branch. To encourage alignment during early timesteps, we introduce a collaborative guidance mechanism where spatial and temporal attention maps from both branches mutually refine each other’s input latents. This mutual alignment enables both branches to align effectively, leading to more coherent integration of customized subjects and their interaction.

As illustrated in Fig. 4(b), given a noised video input  $x_t$ , we duplicate it into  $x_t^{sub}$  and  $x_t^{mot}$  for the subject and motion branches. With  $\hat{\theta}_s$  and  $\theta_m$  denoting the models with the fused subject LoRA and the motion LoRA applied, respectively, we generate *subject* noise ( $\epsilon_t^{sub}$ ) and *motion* noise ( $\epsilon_t^{mot}$ ) as follows:

$$\begin{aligned} \epsilon_t^{sub} &= \epsilon_{\hat{\theta}_s}(x_t^{sub}, c_{tgt}, t), \\ \epsilon_t^{mot} &= \epsilon_{\theta_m}(x_t^{mot}, \tilde{c}_{tgt}, t), \end{aligned} \quad (9)$$

where  $c_{tgt}$  is the input prompt containing subject special tokens (e.g., “A <toy> is riding a <dog>”), and  $\tilde{c}_{tgt}$  is constructed by replacing the special tokens with their respective

superclasses (e.g., “A toy is riding a dog”).

However, since the subject branch (with only subject LoRA) generates incorrect motion, and the motion branch (with only motion LoRA) produces inaccurate spatial arrangements, directly combining  $\epsilon_t^{sub}$  and  $\epsilon_t^{mot}$  might result in incomplete information from either modality. Therefore, we encourage alignment between  $\hat{\theta}_s$  and  $\theta_m$  to produce coherent noise outputs. To achieve this alignment, as depicted in Fig. 4(b), we consider spatial cross-attention maps ( $\mathcal{M}_{SCA}$ ), capturing the spatial arrangement of subjects, and temporal self-attention maps ( $\mathcal{M}_{TSA}$ ), capturing motion dynamics, as demonstrated in previous works [13, 27, 43].

Specifically, we enforce motion correctness by aligning the temporal self-attention maps of the subject branch with those of the motion branch. Similarly, we ensure accurate spatial arrangements by aligning the spatial cross-attention maps of the motion branch with those of the subject branch. Losses for collaborative guidance are calculated as:

$$\begin{aligned} \mathcal{L}_{s \rightarrow m} &= \|\mathcal{M}_{SCA,s} - \mathcal{M}_{SCA,m}\|_2^2, \\ \mathcal{L}_{m \rightarrow s} &= \|\mathcal{M}_{TSA,s} - \mathcal{M}_{TSA,m}\|_2^2, \end{aligned} \quad (10)$$

where the subscripts  $s$  and  $m$  indicate the maps are from

subject and motion branches, respectively. Similar to [1, 5], we update  $x_t^{sub}$  and  $x_t^{mot}$  as follows:

$$\begin{aligned} x_t^{sub} &:= x_t^{sub} - \alpha_t \nabla_{x_t^{sub}} \mathcal{L}_{m \rightarrow s}, \\ x_t^{mot} &:= x_t^{mot} - \alpha_t \nabla_{x_t^{mot}} \mathcal{L}_{s \rightarrow m}, \end{aligned} \quad (11)$$

where  $\alpha_t$  is the step size of the gradient update. This guidance is applied for the first  $\tau$  denoising steps, where  $\tau$  is a hyperparameter. Finally, the predicted noise is calculated by  $\epsilon_t = \beta_s \epsilon_t^{sub} + \beta_m \epsilon_t^{mot}$  where we set  $\beta_s = \beta_m = 0.5$  for simplicity. We leave more details in Algorithm 1 of our supplementary material.

## 4. Experiment

### 4.1. Experimental Setup

**Dataset.** To evaluate video customization methods for multi-subject and motion tasks, we collect 6 motion videos from WebVid [2], featuring various interactions between people and animals. For each motion, we provide 3 subject pairs from [26, 33], including diverse species such as animals, robots, toys, and plushies, with 4 different background prompts per setting.

**Evaluation Metrics.** Following prior works [43, 44, 51], we evaluate performance using: 1) *CLIP-T*, which measures cosine similarity between generated frames and text prompts using CLIP [29]; 2) *CLIP-I*, which assesses subject identity by comparing CLIP image embeddings of generated frames and target images; 3) *DINO-I*, similar to *CLIP-I*, but using embeddings from DINO [4]; 4) *Temporal Consistency* [10], which measures frame-wise consistency by calculating similarity between consecutive frames using CLIP. Additionally, we conduct human evaluations for qualitative assessment.

**Comparisons.** We compare our *VideoMage* with state-of-the-art video customization methods, including DreamVideo [44] and MotionDirector [51], which customize a single subject with motion by applying adapters and LoRAs, respectively. For fair comparisons, we first average the outputs from multiple subject modules and combine them with motion modules for multi-subject and motion customization.

**Implementation Details.** For *VideoMage*, both subject and motion LoRAs are trained for 300 iterations with a rank of 4. We set the learning rates as  $10^{-4}$  for LoRAs and  $10^{-3}$  for textual embeddings. Hyperparameters  $\lambda_1$ ,  $\lambda_2$ , and  $\omega$  are set to 0.25, 0.6, and 0.5, respectively. For SCS,  $\tau = 15$ , and  $\alpha_t$  starts at  $10^4$  and decays by half by the end of denoising, following [5]. For all experiments, we adopt ZeroScope [39] as the video diffusion model. Following [44], we use a 50-step DDIM [37] with a guidance scale of 9.0 to generate

Method	CLIP-T	CLIP-I	DINO-I	T. Cons.
DreamVideo [44]	0.582	0.605	0.197	0.972
MotionDirector [51]	0.656	0.634	0.370	<b>0.987</b>
<b>VideoMage (ours)</b>	<b>0.662</b>	<b>0.670</b>	<b>0.407</b>	0.983

Table 1. **Quantitative comparison on multi-subject and motion customization.** We follow [44, 51] to adopt metrics including CLIP-Text Alignment (*CLIP-T*), CLIP-Image Alignment (*CLIP-I*), DINO-Image Alignment (*DINO-I*), and Temporal Consistency (T. Cons.).

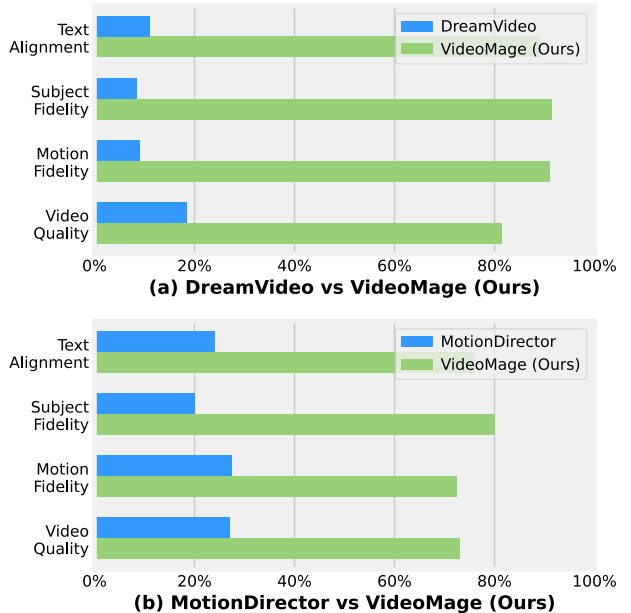


Figure 6. **Human preference study.** Our *VideoMage* consistently achieves the best human preference compared to DreamVideo [44] and MotionDirector [47].

24-frame videos at 8 fps, with a resolution of  $320 \times 576$ . Please refer to the supplementary material for more details.

### 4.2. Main Results

**Qualitative Results.** In Fig. 5, we illustrate examples of customized video generation that combine various user-provided subject images with a specific motion reference video. As we can observe, both DreamVideo and MotionDirector suffer from significant *appearance leakage* and *attribute mixing* issues, struggling to correctly arrange multiple subjects to follow the referenced motion pattern. For instance, in the lower right corner, the black dog’s appearance from the motion video is unintentionally transferred into MotionDirector’s output, while in the DreamVideo’s output in the lower left corner, the color attribute of the <dog> is incorrectly mixed with <robot>, resulting in undesirable visual details. Moreover, both methods fail to establish the

Method	CLIP-T	CLIP-I	DINO-I	T. Cons.
<i>VideoMage</i>	<b>0.662</b>	<b>0.670</b>	<b>0.407</b>	<b>0.983</b>
w/o $\mathcal{L}_{mot}$	0.639	0.651	0.362	0.976
w/o $\mathcal{L}_{attn}$	0.626	0.647	0.358	0.978
w/o SCS	0.601	0.612	0.234	0.982

Table 2. **Quantitative ablation study.** Ablation of our proposed objectives/sampling strategy in *VideoMage*.

intended interactions among subjects, falling short of capturing the nuanced dynamics between them. In contrast, our *VideoMage* effectively addresses these challenges, preserving subject identities, preventing appearance leakage, and successfully achieving the desired interactions between subjects in the generated video.

**Quantitative Results.** We conduct quantitative evaluations on our collected multi-subject and motion dataset (as described in Sec. 4.1). With a total of 72 combinations of subjects, motions, and backgrounds, we generate 10 videos for each combination and evaluate them using four metrics. As shown in Tab. 1, our *VideoMage* generates videos that better preserve the subjects’ identities, outperforming the state-of-the-art method, MotionDirector, by 5.7% and 10% for *CLIP-I* and *DINO-I*, respectively. Additionally, *VideoMage* achieves the highest *CLIP-T* performance and is comparable to SOTA for *Temporal Consistency*, demonstrating its ability to generate coherent videos that align closely with the text prompts.

**User Study.** To further assess the effectiveness of our method, we conduct a human preference study to evaluate our method against DreamVideo [44] and MotionDirector [51]. In this study, participants are given reference subject images and a motion video, along with two customized videos generated by our *VideoMage* and a comparison method, respectively. Participants are asked to choose their preferred video based on four criteria: *Text Alignment* (how well the video matches the prompt), *Subject Fidelity* (how closely the subjects match the reference images without incorrect attribute mixing), *Motion Fidelity* (how accurately the motion reflects the reference video), and *Video Quality* (smoothness and absence of flicker). A total of 360 videos are generated, with 25 participants involved in the evaluation. As shown in Fig. 6, our *VideoMage* was preferred by participants across all criteria.

### 4.3. Ablation Studies

In Fig. 7, we present a qualitative ablation study to analyze the contributions of different components in our proposed *VideoMage*. For the w/o  $\mathcal{L}_{mot}$  setting, we learn the motion pattern using the standard diffusion loss (i.e., Eq. (1)) instead

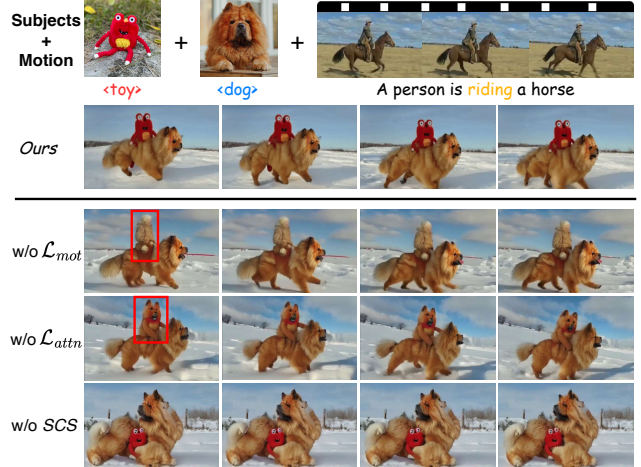


Figure 7. **Ablation study.** Ablation of different components in *VideoMage*. Red boxes indicate appearance leakage or attribute binding issues after removing the specified components.

of the appearance-agnostic objective  $\mathcal{L}_{mot}$ . As a result, we observe severe *appearance leakage*, where the appearance of the person from the reference motion video is unintentionally transferred to the generated output. In the w/o  $\mathcal{L}_{attn}$  setting, we exclude attention regularization during multi-subject fusion, which leads to *attribute binding* issue with mixed attributes between the subjects (e.g., the  $\langle \text{toy} \rangle$  unintentionally looks like a combination of  $\langle \text{toy} \rangle$  and  $\langle \text{dog} \rangle$ ). Lastly, in the w/o SCS setting, we directly combine  $\hat{\theta}_s$  and  $\theta_m$  in the video diffusion model for inference, which struggles to properly arrange subjects with the desired interactive motion. Additionally, we further assess the impact of each of our proposed objectives/modules in Tab. 2. We adopt four metrics to evaluate caption-video similarity (*CLIP-T*), customized subject fidelity (*CLIP-I*, *DINO-I*), and frame-wise consistency (*T. Cons.*). From the above ablation studies, we successfully verify the effectiveness of our designs.

## 5. Conclusion

In this paper, we proposed a unified framework *VideoMage* to enable video customization of text-to-video diffusion models among user-provided subject identities and the desired motion patterns. In *VideoMage*, we employ multi-subject and appearance-agnostic motion learning to derive the customized LoRAs, while presenting a spatial-temporal collaborative composition scheme to mutually align subject and motion components for synthesizing videos with sufficiently visual and temporal fidelity. We conducted extensive quantitative and qualitative evaluations on *VideoMage*, validating its superior controllability over previous video customization methods.

**Acknowledgment** This work is supported in part by the National Science and Technology Council via grant NSTC 113-2634-F-002-005 and NSTC 113-2640-E-002-003, and the Center of Data Intelligence: Technologies, Applications, and Systems, National Taiwan University (grant nos.114L900902, from the Featured Areas Research Center Program within the framework of the Higher Education Sprout Project by the Ministry of Education (MOE) of Taiwan). We also thank the National Center for High-performance Computing (NCHC) for providing computational and storage resources.

## References

- [1] Aishwarya Agarwal, Srikrishna Karanam, KJ Joseph, Apoorv Saxena, Koustava Goswami, and Balaji Vasan Srinivasan. A-star: Test-time attention segregation and retention for text-to-image synthesis. In *ICCV*, pages 2283–2293, 2023. 7
- [2] Max Bain, Arsha Nagrani, Gül Varol, and Andrew Zisserman. Frozen in time: A joint video and image encoder for end-to-end retrieval. In *IEEE International Conference on Computer Vision*, 2021. 7
- [3] Andreas Blattmann, Robin Rombach, Huan Ling, Tim Dockhorn, Seung Wook Kim, Sanja Fidler, and Karsten Kreis. Align your latents: High-resolution video synthesis with latent diffusion models. In *CVPR*, pages 22563–22575, 2023. 2, 3
- [4] Mathilde Caron, Hugo Touvron, Ishan Misra, Hervé Jégou, Julien Mairal, Piotr Bojanowski, and Armand Joulin. Emerging properties in self-supervised vision transformers. In *ICCV*, pages 9650–9660, 2021. 7
- [5] Hila Chefer, Yuval Alaluf, Yael Vinker, Lior Wolf, and Daniel Cohen-Or. Attend-and-excite: Attention-based semantic guidance for text-to-image diffusion models. *ACM TOG*, 42(4): 1–10, 2023. 7
- [6] Hong Chen, Xin Wang, Guanning Zeng, Yipeng Zhang, Yuwei Zhou, Feilin Han, and Wenwu Zhu. Videodreamer: Customized multi-subject text-to-video generation with disenmix finetuning. *arXiv preprint arXiv:2311.00990*, 2023. 2
- [7] Haoxin Chen, Menghan Xia, Yingqing He, Yong Zhang, Xiaodong Cun, Shaoshu Yang, Jinbo Xing, Yaofang Liu, Qifeng Chen, Xintao Wang, et al. Videocrafter1: Open diffusion models for high-quality video generation. *arXiv preprint arXiv:2310.19512*, 2023. 2, 4
- [8] Hong Chen, Xin Wang, Yipeng Zhang, Yuwei Zhou, Zeyang Zhang, Siao Tang, and Wenwu Zhu. Disenstudio: Customized multi-subject text-to-video generation with disentangled spatial control. *arXiv preprint arXiv:2405.12796*, 2024. 2, 12, 13
- [9] Tsai-Shien Chen, Aliaksandr Siarohin, Willi Menapace, Ekaterina Deyneka, Hsiang-wei Chao, Byung Eun Jeon, Yuwei Fang, Hsin-Ying Lee, Jian Ren, Ming-Hsuan Yang, et al. Panda-70m: Captioning 70m videos with multiple cross-modality teachers. In *CVPR*, pages 13320–13331, 2024. 4
- [10] Patrick Esser, Johnathan Chiu, Parmida Atighehchian, Jonathan Granskog, and Anastasis Germanidis. Structure and content-guided video synthesis with diffusion models. In *ICCV*, pages 7346–7356, 2023. 7
- [11] Rinon Gal, Yuval Alaluf, Yuval Atzmon, Or Patashnik, Amit H Bermano, Gal Chechik, and Daniel Cohen-Or. An image is worth one word: Personalizing text-to-image generation using textual inversion. *arXiv preprint arXiv:2208.01618*, 2022. 2, 4, 11
- [12] Rohit Gandikota, Joanna Materzynska, Jaden Fiotto-Kaufman, and David Bau. Erasing concepts from diffusion models. In *ICCV*, pages 2426–2436, 2023. 2, 4
- [13] Yuchao Gu, Xintao Wang, Jay Zhangjie Wu, Yujun Shi, Yunpeng Chen, Zihan Fan, Wuyou Xiao, Rui Zhao, Shuning Chang, Weijia Wu, et al. Mix-of-show: Decentralized low-rank adaptation for multi-concept customization of diffusion models. *NeurIPS*, 36, 2024. 5, 6
- [14] Yuwei Guo, Ceyuan Yang, Anyi Rao, Zhengyang Liang, Yao-hui Wang, Yu Qiao, Maneesh Agrawala, Dahua Lin, and Bo Dai. Animatediff: Animate your personalized text-to-image diffusion models without specific tuning. *arXiv preprint arXiv:2307.04725*, 2023. 2, 3
- [15] Ligong Han, Yinxiao Li, Han Zhang, Peyman Milanfar, Dimitris Metaxas, and Feng Yang. Svdiff: Compact parameter space for diffusion fine-tuning. In *ICCV*, pages 7323–7334, 2023. 5, 11
- [16] Yingqing He, Tianyu Yang, Yong Zhang, Ying Shan, and Qifeng Chen. Latent video diffusion models for high-fidelity long video generation. *arXiv preprint arXiv:2211.13221*, 2022. 2, 3, 4
- [17] Jonathan Ho, Ajay Jain, and Pieter Abbeel. Denoising diffusion probabilistic models. *NeurIPS*, 33:6840–6851, 2020. 1, 3, 4
- [18] Jonathan Ho, William Chan, Chitwan Saharia, Jay Whang, Ruiqi Gao, Alexey Gritsenko, Diederik P Kingma, Ben Poole, Mohammad Norouzi, David J Fleet, et al. Imagen video: High definition video generation with diffusion models. *arXiv preprint arXiv:2210.02303*, 2022. 2, 3
- [19] Jonathan Ho, Tim Salimans, Alexey Gritsenko, William Chan, Mohammad Norouzi, and David J Fleet. Video diffusion models. *NeurIPS*, 35:8633–8646, 2022. 2, 3
- [20] Wenyi Hong, Ming Ding, Wendi Zheng, Xinghan Liu, and Jie Tang. Cogvideo: Large-scale pretraining for text-to-video generation via transformers. *arXiv preprint arXiv:2205.15868*, 2022. 2
- [21] Edward J Hu, Yelong Shen, Phillip Wallis, Zeyuan Allen-Zhu, Yanzhi Li, Shean Wang, Lu Wang, and Weizhu Chen. Lora: Low-rank adaptation of large language models. *arXiv preprint arXiv:2106.09685*, 2021. 2, 3
- [22] Chi-Pin Huang, Kai-Po Chang, Chung-Ting Tsai, Yung-Hsuan Lai, Fu-En Yang, and Yu-Chiang Frank Wang. Receler: Reliable concept erasing of text-to-image diffusion models via lightweight erasers. *arXiv preprint arXiv:2311.17717*, 2023. 2, 4
- [23] Hyeonho Jeong, Geon Yeong Park, and Jong Chul Ye. Vmc: Video motion customization using temporal attention adaptation for text-to-video diffusion models. In *CVPR*, pages 9212–9221, 2024. 2, 3

- [24] Yuming Jiang, Tianxing Wu, Shuai Yang, Chenyang Si, Dahua Lin, Yu Qiao, Chen Change Loy, and Ziwei Liu. Video-booth: Diffusion-based video generation with image prompts. In *CVPR*, pages 6689–6700, 2024. 2, 3
- [25] Diederik P Kingma. Auto-encoding variational bayes. *arXiv preprint arXiv:1312.6114*, 2013. 4
- [26] Nupur Kumari, Bingliang Zhang, Richard Zhang, Eli Shechtman, and Jun-Yan Zhu. Multi-concept customization of text-to-image diffusion. In *CVPR*, pages 1931–1941, 2023. 2, 7
- [27] Pengyang Ling, Jiazi Bu, Pan Zhang, Xiaoyi Dong, Yuhang Zang, Tong Wu, Huaian Chen, Jiaqi Wang, and Yi Jin. Motionclone: Training-free motion cloning for controllable video generation. *arXiv preprint arXiv:2406.05338*, 2024. 6
- [28] Joanna Materzyńska, Josef Sivic, Eli Shechtman, Antonio Torralba, Richard Zhang, and Bryan Russell. Newmove: Customizing text-to-video models with novel motions. In *ACCV*, pages 1634–1651, 2024. 2, 3
- [29] Alec Radford, Jong Wook Kim, Chris Hallacy, Aditya Ramesh, Gabriel Goh, Sandhini Agarwal, Girish Sastry, Amanda Askell, Pamela Mishkin, Jack Clark, et al. Learning transferable visual models from natural language supervision. In *International conference on machine learning*, pages 8748–8763. PMLR, 2021. 7
- [30] Nikhila Ravi, Valentin Gabeur, Yuan-Ting Hu, Ronghang Hu, Chaitanya Ryali, Tengyu Ma, Haitham Khedr, Roman Rädle, Chloe Rolland, Laura Gustafson, et al. Sam 2: Segment anything in images and videos. *arXiv preprint arXiv:2408.00714*, 2024. 5, 11
- [31] Tianhe Ren, Shilong Liu, Ailing Zeng, Jing Lin, Kunchang Li, He Cao, Jiayu Chen, Xinyu Huang, Yukang Chen, Feng Yan, Zhaoyang Zeng, Hao Zhang, Feng Li, Jie Yang, Hongyang Li, Qing Jiang, and Lei Zhang. Grounded sam: Assembling open-world models for diverse visual tasks, 2024. 5, 11
- [32] Yixuan Ren, Yang Zhou, Jimei Yang, Jing Shi, Difan Liu, Feng Liu, Mingi Kwon, and Abhinav Shrivastava. Customize-a-video: One-shot motion customization of text-to-video diffusion models. *arXiv preprint arXiv:2402.14780*, 2024. 2, 3
- [33] Nataniel Ruiz, Yuanzhen Li, Varun Jampani, Yael Pritch, Michael Rubinstein, and Kfir Aberman. Dreambooth: Fine tuning text-to-image diffusion models for subject-driven generation. In *CVPR*, pages 22500–22510, 2023. 2, 7
- [34] Masaki Saito, Eiichi Matsumoto, and Shunta Saito. Temporal generative adversarial nets with singular value clipping. In *ICCV*, pages 2830–2839, 2017. 2
- [35] Uriel Singer, Adam Polyak, Thomas Hayes, Xi Yin, Jie An, Songyang Zhang, Qiyuan Hu, Harry Yang, Oron Ashual, Oran Gafni, et al. Make-a-video: Text-to-video generation without text-video data. *arXiv preprint arXiv:2209.14792*, 2022. 2, 3
- [36] Ivan Skorokhodov, Sergey Tulyakov, and Mohamed Elhoseiny. Stylegan-v: A continuous video generator with the price, image quality and perks of stylegan2. In *CVPR*, pages 3626–3636, 2022. 2
- [37] Jiaming Song, Chenlin Meng, and Stefano Ermon. Denoising diffusion implicit models. *arXiv preprint arXiv:2010.02502*, 2020. 1, 7, 12
- [38] Yang Song, Jascha Sohl-Dickstein, Diederik P Kingma, Abhishek Kumar, Stefano Ermon, and Ben Poole. Score-based generative modeling through stochastic differential equations. *arXiv preprint arXiv:2011.13456*, 2020. 1
- [39] Spencer Sterling. Zeroscope. [https://huggingface.co/cerspense/zeroscope\\_v2\\_576w](https://huggingface.co/cerspense/zeroscope_v2_576w), 2023. 2, 7
- [40] Sergey Tulyakov, Ming-Yu Liu, Xiaodong Yang, and Jan Kautz. Mocogan: Decomposing motion and content for video generation. In *CVPR*, pages 1526–1535, 2018. 2
- [41] Carl Vondrick, Hamed Pirsiavash, and Antonio Torralba. Generating videos with scene dynamics. *NeurIPS*, 29, 2016. 2
- [42] Jiuniu Wang, Hangjie Yuan, Dayou Chen, Yingya Zhang, Xiang Wang, and Shiwei Zhang. Modelscope text-to-video technical report. *arXiv preprint arXiv:2308.06571*, 2023. 2, 4
- [43] Zhao Wang, Aoxue Li, Enze Xie, Lingting Zhu, Yong Guo, Qi Dou, and Zhenguo Li. Customvideo: Customizing text-to-video generation with multiple subjects. *arXiv preprint arXiv:2401.09962*, 2024. 2, 3, 6, 7, 12, 13
- [44] Yujie Wei, Shiwei Zhang, Zhiwu Qing, Hangjie Yuan, Zhiheng Liu, Yu Liu, Yingya Zhang, Jingren Zhou, and Hongming Shan. Dreamvideo: Composing your dream videos with customized subject and motion. In *CVPR*, pages 6537–6549, 2024. 2, 3, 6, 7, 8, 12
- [45] Dirk Weissenborn, Oscar Täckström, and Jakob Uszkoreit. Scaling autoregressive video models. *arXiv preprint arXiv:1906.02634*, 2019. 2
- [46] Chenfei Wu, Lun Huang, Qianxi Zhang, Binyang Li, Lei Ji, Fan Yang, Guillermo Sapiro, and Nan Duan. Godiva: Generating open-domain videos from natural descriptions. *arXiv preprint arXiv:2104.14806*, 2021. 2
- [47] Jianzong Wu, Xiangtai Li, Yanhong Zeng, Jiangning Zhang, Qianyu Zhou, Yining Li, Yunhai Tong, and Kai Chen. Motionbooth: Motion-aware customized text-to-video generation. *arXiv preprint arXiv:2406.17758*, 2024. 3, 4, 7
- [48] Yen-Siang Wu, Chi-Pin Huang, Fu-En Yang, and Yu-Chiang Frank Wang. Motionmatcher: Motion customization of text-to-video diffusion models via motion feature matching. *arXiv preprint arXiv:2502.13234*, 2025. 2, 3
- [49] Wilson Yan, Yunzhi Zhang, Pieter Abbeel, and Aravind Srivas. Videogpt: Video generation using vq-vae and transformers. *arXiv preprint arXiv:2104.10157*, 2021. 2
- [50] Sangdoon Yun, Dongyoon Han, Seong Joon Oh, Sanghyuk Chun, Junsuk Choe, and Youngjoon Yoo. Cutmix: Regularization strategy to train strong classifiers with localizable features. In *ICCV*, pages 6023–6032, 2019. 5, 11
- [51] Rui Zhao, Yuchao Gu, Jay Zhangjie Wu, David Junhao Zhang, Jiawei Liu, Weijia Wu, Jussi Keppo, and Mike Zheng Shou. Motiondirector: Motion customization of text-to-video diffusion models. *arXiv preprint arXiv:2310.08465*, 2023. 2, 3, 6, 7, 8, 12



# VideoMage: Multi-Subject and Motion Customization of Text-to-Video Diffusion Models

## Supplementary Material

### 6. Limitation and Future Work

While our method effectively customizes multiple subjects and their motions in videos, it currently lacks the capability to customize long motions and generate corresponding extended videos (e.g., minute-long videos). This limitation is common across all existing methods, as customizing longer videos requires significant computational resources, either during training or inference.

To address this, future work will explore integrating long video generation techniques or training-free customization methods to enable longer customized video generation. By leveraging advancements in efficient video synthesis capable of handling long video sequences, we aim to improve the generation of longer and more intricate customized video content.

### 7. Additional Experimental Setup

#### 7.1. Additional Implementation Details

**Appearance-Agnostic Motion Learning.** As described in Sec. 3.2, we employ Textual Inversion [11] to obtain the special tokens representing subject appearances from the ref-

---

#### Algorithm 1 Spatial-Temporal Collaborative Sampling (SCS)

---

**Model:** Pre-trained video diffusion model  $\theta$ , fused multi-subject LoRA  $\Delta\hat{\theta}_s$ , motion LoRA  $\Delta\theta_m$

**Input:** Target text prompt  $c_{tgt}$  (w/ subjects' special tokens) and  $\tilde{c}_{tgt}$  (w/o special tokens), initial noise map  $x_T$

**Output:** Sampled video  $x_0$

```

1: for  $t = T, T - 1, \dots, 1$  do
2:   Duplicate  $x_t$  to create  $x_t^{sub}$  and  $x_t^{mot}$ ;
3:    $\epsilon_t^{sub} = \epsilon_{\hat{\theta}_s}(x_t^{sub}, c_{tgt}, t)$ ;   {Subject branch noise}
4:    $\epsilon_t^{mot} = \epsilon_{\theta_m}(x_t^{mot}, \tilde{c}_{tgt}, t)$ ;   {Motion branch noise}
5:   if  $T - t < \tau$  then
6:     /* Collaborative Guidance */
7:      $\mathcal{L}_{s \rightarrow m} = \|\mathcal{M}_{SCA,s} - \mathcal{M}_{SCA,m}\|_2^2$ ;
8:      $\mathcal{L}_{m \rightarrow s} = \|\mathcal{M}_{TSA,s} - \mathcal{M}_{TSA,m}\|_2^2$ ;
9:      $x_t^{sub} := x_t^{sub} - \alpha_t \nabla_{x_t^{sub}} \mathcal{L}_{m \rightarrow s}$ ;
10:     $x_t^{mot} := x_t^{mot} - \alpha_t \nabla_{x_t^{mot}} \mathcal{L}_{s \rightarrow m}$ ;
11:    Execute lines 3 and 4 to get updated  $\epsilon_t^{sub}$  and  $\epsilon_t^{mot}$ ;
12:  end if
13:   $\epsilon_t = \beta_s \epsilon_t^{sub} + \beta_m \epsilon_t^{mot}$  and obtain  $x_{t-1}$ ;
14: end for
15: Return  $x_0$ ;

```

---



1. Which video has **motion** most similar to the target video?
 

Video 1  Video 2
2. Which video contains **subjects** most similar to those in the target images?
 

Video 1  Video 2
3. Which video better matches the **text description**?  
 "robot is walking cat in the city."
 

Video 1  Video 2
4. Which video is smoother and has less flicker?
 

Video 1  Video 2

Figure 8. **User study interface.** Given two generated videos, reference subject images, and a reference motion video, participants compare the generated videos based on *Motion Fidelity*, *Subject Fidelity*, *Text Alignment*, and *Video Quality*.

erence motion video for our proposed *appearance-agnostic motion learning*. Specifically, we extract a single frame from the reference video and use Grounded-SAM [31] to obtain segmentation masks for each subject. We then crop each subject based on its corresponding mask and learn a special token (i.e., embedding) for each subject using Eq. (4). This approach ensures that the learned tokens accurately reflect the visual identities of the subjects without incorporating any motion information, which is crucial for the appearance-agnostic motion learning phase.

**Spatial-Temporal Collaborative Composition.** As mentioned in Sec. 3.3, we sample and preprocess two single-subject training videos by combining them into a CutMix-style [15, 50] video for regularizing the LoRA fusion. Specifically, for each video, we use Grounded-SAM2 [30, 31] to generate segmentation masks for the subjects. We then crop

$\lambda_1$	CLIP-T	CLIP-I	DINO-I	T. Cons.
0.1	0.658	0.667	0.398	0.981
0.25	<b>0.662</b>	<b>0.670</b>	<b>0.407</b>	<b>0.983</b>
1.0	0.660	0.667	0.401	0.980

(a) Weight for video preservation loss  $\lambda_1$ 

Template for $c_{ap}$	CLIP-I	DINO-I
“A static video of <sub1> and <sub2>.”	<b>0.670</b>	<b>0.407</b>
“A video of <sub1> and <sub2> being still.”	0.664	0.405
“A video of <sub1> and <sub2>.”	0.659	0.395

(c) Template for appearance prompt  $c_{ap}$ 

$\alpha_t$	CLIP-T	CLIP-I	DINO-I	T. Cons.
$10^3$	0.657	0.665	0.401	<b>0.988</b>
$10^4$	<b>0.662</b>	<b>0.670</b>	<b>0.407</b>	0.983
$10^5$	0.634	0.658	0.379	0.976

(e) Scale factor of collaborative guidance  $\alpha_t$ 

$\lambda_2$	CLIP-T	CLIP-I	DINO-I	T. Cons.
0.1	0.641	0.659	0.362	0.980
0.6	<b>0.662</b>	<b>0.670</b>	<b>0.407</b>	0.983
1.0	0.656	0.665	0.402	<b>0.984</b>

(b) Weight for attention regularization loss  $\lambda_2$ 

$\omega$	CLIP-T	CLIP-I	DINO-I	T. Cons.
0.1	0.646	0.658	0.372	0.981
0.5	<b>0.662</b>	<b>0.670</b>	<b>0.407</b>	<b>0.983</b>
1.0	0.657	0.667	0.403	0.980

(d) Scale factor of negative guidance  $\omega$ 

$\tau$	CLIP-T	CLIP-I	DINO-I	T. Cons.
5	0.658	0.664	0.401	0.978
15	<b>0.662</b>	<b>0.670</b>	<b>0.407</b>	<b>0.983</b>
30	0.657	0.664	0.399	0.975

(f) Steps of collaborative guidance  $\tau$ Table 3. Ablation studies on various hyperparameters, including the weights for video preservation loss ( $\lambda_1$ ) and attention regularization loss ( $\lambda_2$ ), the template for appearance prompt ( $c_{ap}$ ), the negative guidance scale factor ( $\omega$ ), the collaborative guidance scale ( $\alpha_t$ ) and steps ( $\tau$ ).

the subjects from the original frames and place them onto a clean background video. To encourage potential interactions between the subjects, we allow some degree of overlap in their placements. We initialize the fused LoRA  $\hat{\theta}_s$  with the average of the subject LoRAs. The training steps range from 250 to 450, depending on the subject combination.

For *spatial-temporal collaborative sampling* (SCS), we provide the details in Algorithm 1. Following prior works [44, 51], we initialize the noise map as  $x_T = \sqrt{\beta}\epsilon_m + \sqrt{1-\beta}\epsilon$ , where  $\beta = 0.3$ ,  $\epsilon_m$  is the DDIM [37] inverted noise of the motion video, and  $\epsilon$  is Gaussian noise sampled from  $\mathcal{N}(\mathbf{0}, \mathbf{I})$ . This initialization is consistently applied to all comparison methods in all experiments.

## 7.2. Human User Study

In Fig. 8, we present the interface for our human preference study. In this study, participants are provided with reference subject images, a reference motion video, and two customized videos: one from our *VideoMage* method and one from a comparison method (i.e., DreamVideo [44] or MotionDirector [51]). They are asked to choose their preferred video based on four questions, each evaluating: *Motion Fidelity*, *Subject Fidelity*, *Text Alignment*, and *Video Quality*. A total of 360 videos were generated for each method, and 25 participants participated in the study.

## 8. Additional Results

### 8.1. Ablation Studies on Hyperparameter Choices

**Effect of  $\lambda_1$  in subject learning.** As illustrated in Tab. 3(a), a video preservation loss weight of  $\lambda_1 = 0.25$  achieves the best performance, while both smaller (0.1) and larger (1.0)

Method	CLIP-T	CLIP-I	DINO-I	T. Cons.
DisenStudio [8]	0.661	0.658	0.381	0.842
CustomVideo [43]	<b>0.676</b>	0.679	0.402	0.849
<b>VideoMage (ours)</b>	0.674	<b>0.681</b>	<b>0.403</b>	<b>0.851</b>

Table 4. **Quantitative comparison on multi-subject customization.** Following [8, 43], we evaluate using CLIP-Text Alignment (*CLIP-T*), CLIP-Image Alignment (*CLIP-I*), DINO-Image Alignment (*DINO-I*), and Temporal Consistency (T. Cons.).

values lead to declines. Thus, we set  $\lambda_1 = 0.25$  for all experiments.

**Effect of  $\lambda_2$  in multi-subject fusion.** As shown in Tab. 3(b), the optimal performance is achieved with the attention regularization loss weight set to  $\lambda_2 = 0.6$ , whereas smaller (0.1) or larger (1.0) values lead to reduced performance. Thus, we use  $\lambda_2 = 0.6$  in our experiments.

**Effect of  $c_{ap}$  and  $\omega$  in appearance-agnostic motion learning.** As shown in Tab. 3(c), we experiment with three different templates for the subject appearance prompt  $c_{ap}$  used in our appearance-agnostic motion learning. The template, “A static video of <sub1> and <sub2>,” achieves the best performance and is therefore used in our experiments. Notably, all three templates outperform the second-best result achieved by MotionDirector [51], as presented in Tab. 1. Similarly, in Tab. 3(d), we present the ablation study on the scale factor of negative guidance  $\omega$ . We observe that setting  $\omega$  to 0.5 yields the best results; thus,  $\omega = 0.5$  is adopted for all experiments.

**Effect of  $\tau$  and  $\alpha_t$  in spatial-temporal collaborative sampling.** In Tab. 3(e) and Tab. 3(f), we ablate the scale factor  $\alpha_t$  and steps  $\tau$  in our proposed spatial-temporal collaborative sampling, respectively. As shown in Tab. 3(e), increasing  $\alpha_t$  from  $10^3$  to  $10^4$  improves performance, but further increasing it to  $10^5$  results in a decline. Consequently, we set  $\alpha_t = 10^4$  for our experiments. Similarly, in Tab. 3(f), increasing  $\tau$  to 15 improves performance, while any further increase leads to a drop. Therefore, we set  $\tau = 15$ .

## 8.2. Multi-Subject Customization

To validate the effectiveness of our proposed *test-time multi-subject fusion*, we compare *VideoMage* with state-of-the-art methods on the multi-subject customization task. Using the subject sets and prompts described in Sec. 4.1, we generate 720 videos and evaluate performance using *CLIP-T*, *CLIP-I*, *DINO-I*, and *T. Cons.*, following [8, 43]. For fair comparison, we omit the additional bounding boxes required by DisenStudio. As shown in Tab. 4, *VideoMage* outperforms the second-best method in *CLIP-I*, *DINO-I*, and *T. Cons.*, and is comparable to CustomVideo in *CLIP-T*.

## 8.3. More Qualitative Results.

In Fig. 9, we present additional qualitative results of *VideoMage* customizing videos with multiple subjects and motion, successfully demonstrating diverse subject-motion combinations across various scenes, including cases with more than two subjects.



Figure 9. **Additional qualitative results.** Each row presents the subject images, the motion video, the corresponding customized video results, and the input prompt.